Dynamin 2 orchestrates the global actomyosin cytoskeleton for epithelial maintenance and apical constriction

Jennifer Chua, Richa Rikhy, and Jennifer Lippincott-Schwartz[1]

Cell Biology and Metabolism Program, National Institute of Child Health and Human Development, National Institutes of Health, Bethesda, MD 20892

Contributed by Jennifer Lippincott-Schwartz, September 9, 2009 (sent for review July 16, 2009)

The mechanisms controlling cell shape changes within epithelial monolayers for tissue formation and reorganization remain unclear. Here, we investigate the role of dynamin, a large GTPase, in epithelial morphogenesis. Depletion of dynamin 2 (Dyn2), the only dynamin in epithelial cells, prevents establishment and maintenance of epithelial polarity, with no junctional formation and abnormal actin organization. Expression of Dyn2 mutants shifted to a non-GTP state, by contrast, causes dramatic apical constriction without disrupting polarity. This is due to Dyn2's interactions with deacetylated cortactin and downstream effectors, which cause enhanced actomyosin contraction. Neither inhibitors of endocytosis nor GTP-shifted Dyn2 mutants induce apical constriction. This suggests that GTPase-dependent changes in Dyn2 lead to interactions with different effectors that may differentially modulate endocytosis and/or actomyosin dynamics in polarized cells. We propose this enables Dyn2 to coordinate, in a GTPase-dependent manner, membrane recycling and actomyosin contractility during epithelial morphogenesis.

deacetylated cortactin | actin | polarity | morphogenesis | epithelial cells

A key property of epithelium is that small changes in cell shape within individual cells collectively generate large-scale tissue reorganization (1). This plays an important role in determining the final shape and form of an organism. For example, conversion of a few cells into wedge-like shapes within an epithelium through constriction of the cell's apical domain can convert flat epithelial sheets into folded and tubule forms (2). The resulting bending and remodeling of the epithelium underlies many complex morphogenic pathways, including gastrulation and neural tube closure (2, 3).

Coordination between membrane remodeling and actin dynamics is known to be important for epithelial morphogenesis (4, 5). In addition, the formation of dynamic arrays of apical junctional complexes helps compartmentalize cells within the epithelium and allows the monolayer to be responsive to different stimuli (5). For example, tight junctional proteins form homophilic interactions between adjacent cells, segregating the epithelium into basolateral and apical surfaces, whereas adherens junctional proteins, located adjacent to tight junctions, participate in cell–cell adhesion and cell packing (4). The junctional proteins are linked to the actin cytoskeleton by interactions with proteins associated with the inner plasma membrane (4). This helps the epithelium to retain and/or alter its shape and to maintain membrane tension across itself. The pool of apical junctional complexes at the subapical plasma membrane region is dynamically maintained, with complexes continually being removed by endocytosis and replenished from internal stores (6).

The large GTPase dynamin, which functions in both endocytic membrane remodeling and cytoskeletal regulation (7–9), is a potential candidate for regulating epithelial morphogenesis. Dynamin contains an N-terminal GTPase domain, a pleckstrin homology (PH) domain, a middle domain, a GTPase effector domain (GED) important for oligomerization, and a C-terminal proline-rich domain (PRD) capable of interacting with a wide variety of SH3 domain-containing proteins (7, 8). A key property of dynamin is that it self-assembles into ordered polymers that undergo conformational changes when GTP is hydrolyzed (10). This occurs concurrently with actin filament remodeling because of dynamin's ability to bind different proteins that link membranes to the cytoskeleton, including membrane curvature-sensing proteins, scaffolding proteins that link to nucleating factors, and other actin-binding proteins (7, 9). By functioning as a polymeric contractile scaffold with many partners, dynamin is able to deform membranes and orchestrate actin filament assembly at the plasma membrane for regulation of many processes, including endocytic uptake, vesicle movement, podosomal activity, and cell migration (9).

Because of dynamin's dual functions in membrane remodeling and actin regulation, we investigated its role in epithelial morphogenesis. Here, we show that dynamin 2 (Dyn2), the only form in epithelial cells, both regulates endocytosis and contributes to maintaining a normal and dynamic actomyosin array at the apical junctional surface, presumably via effects on cytoskeletal effectors and/or interacting partners.

Results

Formation and Maintenance of Polarized Epithelial Monolayers Requires Dyn2. The effect of Dyn2 depletion on monolayer formation was examined by subjecting suspended MDCK cells to Dyn2 or control siRNA transfection. Western blot analysis showed that >93.2% of Dyn2 expression was lost after Dyn2 siRNA treatment (Fig. 1*A*). In control siRNA-treated cells, the membrane-associated, tight junctional marker, ZO-1, labeled the junctional belt surrounding each cell (Fig. 1*B*). Actin stress fibers, observed by Texas Red (TxRed)-phalloidin labeling, showed a basal and lateral organization (Fig. 1*B*). In Dyn2 siRNA-treated cells, by contrast, ZO-1 labeling was absent or seen in puncta (Fig. 1*B*), indicating junctional complexes did not assemble and actin stress fibers were now only on lateral membranes (Fig. 1*B*). In the absence of Dyn2, therefore, epithelial cells that are newly plated in culture chambers do not polarize properly.

To test the effect of Dyn2 depletion on fully polarized epithelial monolayers, we treated preformed monolayers with control or Dyn2 siRNA and then labeled for ZO-1 (Fig. 1*C*). A cobblestone pattern of ZO-1 staining, indicative of normal monolayer morphology, was seen in control siRNA-treated cells. A discontinuous ZO-1 staining, suggestive of tight junction disruption, was seen in Dyn2 siRNA-treated cells, with nontransfected cells in the same monolayer continuing to exhibit normal polygonal morphology. Dyn2 is

Author contributions: J.C. and J.L.-S. designed research; J.C. and R.R. performed research; J.C. and R.R. contributed new reagents/analytic tools; J.C., R.R., and J.L.-S. analyzed data; and J.C. and J.L.-S. wrote the paper.

The authors declare no conflict of interest.

Freely available online through the PNAS open access option.

See Commentary on page 20559.

[1]To whom correspondence should be addressed. E-mail: JLippin@helix.nih.gov.

This article contains supporting information online at www.pnas.org/cgi/content/full/0909812106/DCSupplemental.

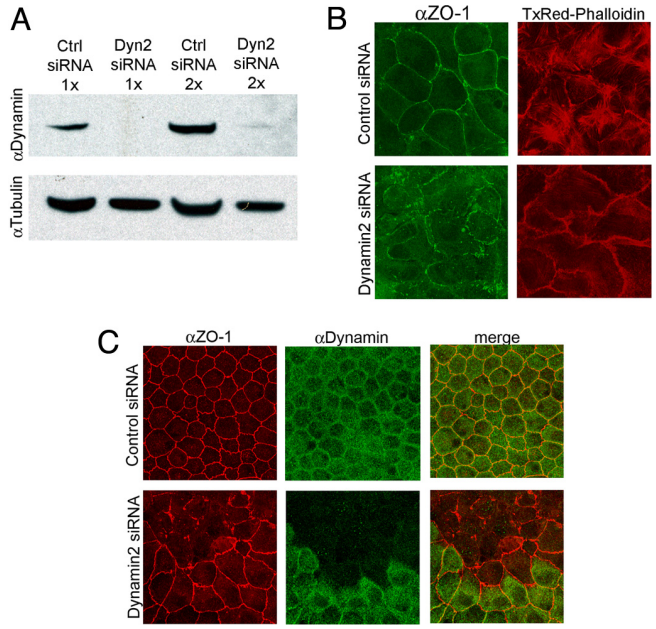

Fig. 1. Dyn2-targeted siRNA inhibits epithelial monolayer formation and maintenance. (*A*) Blot analysis of cell lysate from MDCK cells transfected with Dyn2 or control siRNA. 1× or 2× indicates the number of times cells were subjected to siRNA transfection. (*B*) Maximum-intensity projection images of monolayers formed after transfection of MDCK cells in suspension with either control (*Upper*) or Dyn2 (*Lower*) siRNA and stained for ZO-1 (green) and actin (red). Note the severely disrupted tight junctions, increase in actin lateral staining, and lack of stress fibers in Dyn2 siRNA-treated cells. (*C*) Maximum intensity projection images of MDCK cells transfected in preformed monolayers with either control (*Upper*) or Dyn2 siRNA (*Lower*) and stained for ZO-1 (red) and Dynamin (green). Note the severely disrupted tight junctions in cells that do not stain for dynamin (*Lower*).

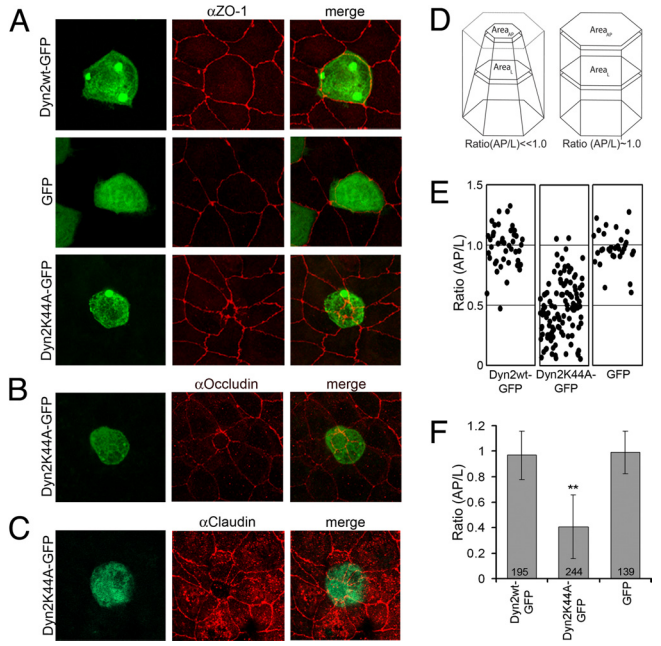

Fig. 2. Apical constriction is induced by Dyn2K44A expression. (*A–C*) Maximum intensity projection images of monolayers transfected with Dyn2wt-GFP (*A Top*), GFP (*A Middle*), or Dyn2K44A-GFP (*A Bottom*, *B*, and *C*) and stained for ZO-1 (*A*), occludin (*B*), or claudin (*C*). Note constriction of the junctional belt in *A Bottom*, *B*, and *C*. (*D*) Schematic diagram of epithelial cells having undergone apical constriction (*Left*) or with normal morphology (*Right*). Ratio (AP/L) = the ratio of the apical area relative to an area of the lateral cross-section 1–2 μm below the AJC. (*E*) Distributions of individual ratio values in cells expressing Dyn2wt-GFP, Dyn2K44A-GFP, or GFP from three separate experiments. (*F*) Mean ratio (AP/L) in cells transfected with Dyn2wt-GFP, Dyn2K44A-GFP, or GFP from eight separate experiments. **, $P < 0.001$.

thus necessary for both the initiation and maintenance of epithelial polarity in MDCK cell monolayers.

Dyn2K44A Expression Induces Apical Constriction in Polarized Epithelial Cells. Epithelial morphology was next examined in cells expressing a Dyn2 mutant unable to efficiently bind GTP, known as Dyn2K44A (11). MDCK cells grown on Transwells were transfected with (*i*) GFP-tagged Dyn2K44A (Dyn2K44A-GFP), (*ii*) GFP-tagged Dyn2 wild-type (Dyn2wt-GFP), or (*iii*) GFP alone. The monolayers were then stained for various junctional markers to assess tight-junctional morphology. In cells expressing Dyn2wt-GFP or GFP alone, normal epithelial polygonal morphology occurred with the junctional belt (revealed by ZO-1 labeling) roughly the same size as the cytoplasmic volume (revealed by GFP labeling; Fig. 2*A*). By contrast, in Dyn2K44A-GFP-expressing cells, the junctional belt dramatically constricted relative to the cytoplasmic volume, as revealed by ZO-1, occludin, and claudin staining (Fig. 2 *A–C*). The Dyn2K44A-GFP-expressing cells resembled an inverted cone or bottle, with the apical surface much smaller than the lateral cross-sectional and basal area (Movie S1), in contrast to the columnar shape of Dyn2wt-GFP-expressing (Movie S2) or GFP-expressing cells (Movie S3).

We quantified apical constriction by measuring the apical surface area and dividing it by the lateral cross-sectional area 1–3 μm below the plane of the apical junctional complex. Cells with normal columnar morphology should display an apical to lateral (AP/L) ratio of 1.0, whereas apically constricted cells should have AP/L ratios much lower than 1.0 (Fig. 2*D*). The average AP/L ratios in Dyn2wt-GFP-expressing (0.97 ± 0.19) and GFP-expressing (0.99 ± 0.17) cells were close to 1.0, whereas in Dyn2K44A-GFP-expressing cells, the average AP/L ratio was 0.41 ± 0.25, indicative of apical constriction (Fig. 2 *E* and *F*). Hence, rather than abolishing epithelial polarity, as seen with Dyn2 depletion, Dyn2K44A expression gave rise to a new phenotype—apical constriction.

Tight Junctional Integrity and Polarity Are Retained in Apically Constricted Cells Induced by Dyn2K44A Expression. To investigate whether epithelial polarity is disrupted in Dyn2K44A-expressing cells, we visualized the distribution of a variety of apical and basolateral markers and compared it to Dyn2wt-expressing cells, which served as a control. We found the basolateral protein marker, Na^+ taurocholate cotransporting polypeptide tagged with GFP (NTCP-GFP) (12), was primarily basolateral in both Dyn2K44A-RFP-expressing and Dyn2wt-RFP-expressing cells (Fig. S1*A*). Likewise, the apical lipid marker, PLCδ PH-GFP (13), was predominantly apical in both types of expressing cells (Fig. S1*B*). The adherens junctional protein, E-cadherin, was observed in lateral membranes in both types of expressing cells (Fig. S1*C*). Immunostaining for ezrin, an apically localized microvillus protein, showed restricted apical labeling in both Dyn2K44A-GFP-expressing and Dyn2wt-GFP-expressing cells (Fig. S1*D*). Finally, adding the lipophilic dye FM4-64 to basolateral membranes of Dyn2K44A-GFP-expressing or Dyn2wt-GFP expressing cells revealed dye retention on basolateral surfaces in both conditions, with no diffusion occurring across tight junctions to apical membranes (Fig. S1*E*). Apically constricted, Dyn2K44A-expressing cells thus maintain tight junctional integrity and the polarized distribution of apical and basolateral markers.

Blocking Endocytosis Does not Induce Apical Constriction in Monolayers. Neither TxRed-transferrin or TxRed-dextran was endocytosed in Dyn2K44A-expressing cells (Fig. 3 *A* and *B*). We investigated, therefore, whether the apical constriction phenotype induced

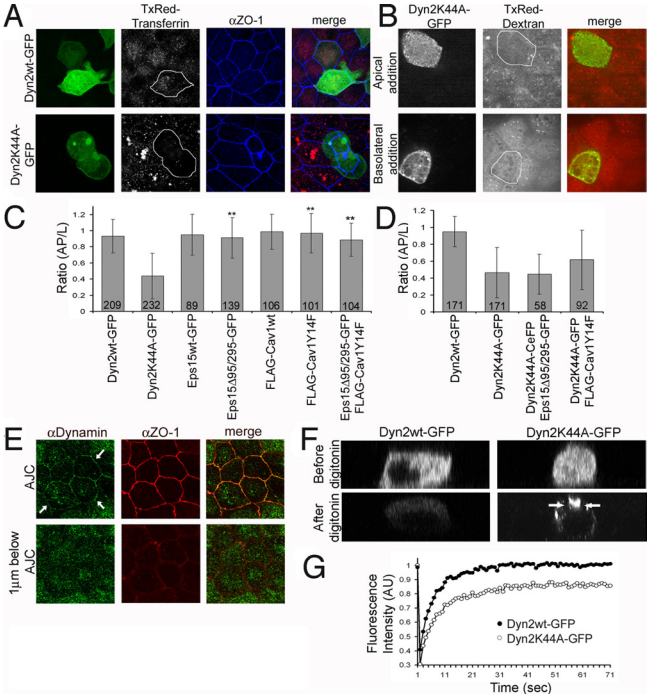

Fig. 3. Apical constriction is not due to inhibiting endocytosis, and dynamin is enriched at the apical junctional region. (*A*) Maximum intensity projection images of cells expressing Dyn2wt-GFP (*Left Upper*, green) and Dyn2K44A-GFP (*Left Lower*, green) that were incubated with TxRed-transferrin (red) and stained for ZO-1 (blue). (*B*) Single plane images taken below AJC of Dyn2K44A-GFP-expressing cells subjected to TxRed-dextran applied either apically or basolaterally and imaged live. (*C*) Mean ratio (AP/L) for cells expressing Dyn2wt-GFP, Dyn2K44A-GFP, Eps15wt-GFP, Eps15Δ95/295-GFP, FLAG-Cav1wt, FLAG-Cav1Y14F, or Eps15Δ95/295-GFP and FLAG-Cav1Y14F in at least three separate experiments. **, $P < 0.001$. (*D*) Mean ratio (AP/L) for cells expressing Dyn2wt-GFP, Dyn2K44A-GFP, Dyn2K44A-CeFP, and Eps15Δ95/295-GFP, or Dyn2K44A-GFP and FLAG-Cav1Y14F from two independent experiments. (*E*) Single-plane images of a monolayer stained for dynamin (green) and ZO-1 (red) at the AJC (*Upper*) and 1 μm below the AJC (*Lower*). Note dynamin enrichment (arrows) at the AJC but not at the basolateral membranes. (*F*) XZ sections of cells expressing Dyn2wt-GFP (*Left*) and Dyn2K44A-GFP (*Right*) before and after treatment with 0.01% digitonin. Note the enrichment of Dyn2K44A-GFP relative to Dyn2wt-GFP (arrows). (*G*) FRAP recovery kinetics for Dyn2wt-GFP and Dyn2K44A-GFP in cells expressing an individual chimera.

by Dyn2K44A expression was due to this endocytosis block. Other conditions that block endocytosis were examined to see whether they induced apical constriction in MDCK cells. The conditions tested included: expression of a truncated form of Eps15 (Eps15Δ95/295), which prevents AP-2 recruitment to membranes (14); expression of a caveolin mutant defective in phosphorylation (Cav1Y14F) that prevents caveolae-mediated internalization (15); and coexpression of both. Quantification of AP/L ratios for cells under each condition reveals a ratio close to that seen for Dyn2wt, indicating most cells did not become apically constricted (Fig. 3*C*), despite having endocytosis inhibited. Apical constriction induced by Dyn2K44A expression, furthermore, was still observed when cells coexpressed Eps15Δ95/295-GFP or FLAG-Cav1Y14F (Fig. 3*D*). Together, these results suggest that apical constriction induced by Dyn2K44A is not a general consequence of inhibiting endocytosis.

Dynamin Localization and Dynamics Are Changed in Dyn2K44A-Expressing Cells. The distribution and dynamics of Dyn2K44A expressed in MDCK cells were next studied to gain clues as to how this mutant might function to drive apical constriction. We began by examining the distribution of endogenous Dyn2 stained with antibodies (Fig. 3*E*). The antibody labels plasma membranes primarily in the apical junctional region of nontransfected MDCK cells, colocalizing with ZO-1. Note there was no Dyn2 and ZO-1 membrane labeling in the next confocal section below the junctional plane. Besides this membrane localization, immunolocalized Dyn2 was seen diffusely in the cytoplasm and in association with intracellular structures, most likely the Golgi apparatus, as previously reported (17).

We next used confocal Z sectioning to examine the distribution of Dyn2wt-GFP and Dyn2K44A-GFP in MDCK cells. Dyn2wt-GFP had a distribution similar to that of Dyn antibody labeling, with the chimera slightly enriched on apical junctional membranes and found on puncta or dispersed in the cytoplasm (Fig. S2*A*, arrows). The distribution of Dyn2K44A-GFP superficially resembled that of Dyn2wt-GFP, except it had a more intense membrane association at the junctional region (Fig. S2*B*, arrows). To test whether this resulted from Dyn2K44A-GFP being more retained at the apical junctional area than Dyn2wt-GFP, we permeabilized living cells with a mild digitonin treatment to allow freely diffusing forms of the constructs to be released from cells. Whereas most Dyn2wt-GFP was lost by this treatment, a large fraction of cellular Dyn2K44A-GFP remained, particularly the pool localized at the junctional region (Fig. 3*F*).

We photobleached the apical junctional area of MDCK cells containing Dyn2wt-GFP or Dyn2K44A-GFP to investigate the fluorescence recovery from surrounding areas and the presence of immobile protein pools. In Dyn2wt-GFP-expressing cells, complete recovery of fluorescence occurred in less than 30 sec, indicating the chimera undergoes rapid movement in and out of the junctional region (Fig. 3*G* and Fig. S2*C*). In Dyn2K44A-expressing cells, by contrast, recovery was slower, and there was a significant immobile fraction. Hence, Dyn2K44A associates more tightly with the apical junctional area of epithelial cells than wild-type Dyn2.

Apical Constriction in Dyn2K44A-Expressing Cells Occurs by a Rho-Dependent, Myosin II Pathway. Apical constriction is driven by an actomyosin contractile system (18), so a way that Dyn2K44A expression might drive constriction is if its increased accumulation in this area triggers contraction. Consistent with this possibility, we found that both actin (labeled using TxRed-phalloidin; Fig. 4*A*) and myosin II (labeled using antibodies; Fig. 4*B*) were dramatically increased in the apical domain of constricted cells. Moreover, perturbing the actin cytoskeleton through treatment with cytochalasin D (which inhibits actin polymerization) or jasplakinolide (which stabilizes actin) reverted the apical constriction phenotype seen in Dyn2K44A-GFP-expressing cells back to normal morphology (Fig. 4*C*). This indicates that actin polymerization and depolymerization are necessary to form and maintain the apical constriction phenotype. In contrast, no relief of apical constriction was observed in Dyn2K44A-GFP-expressing cells treated with microtubule-depolymerizing reagents, including nocodazole and demecolcine, after a cold treatment (Fig. 4*D*). Furthermore, treatment with blebbistatin, which inhibits myosin II ATPase motor activity, reverted the constricted phenotype in Dyn2K44A-GFP-expressing cells, with no morphological effect on nonexpressing cells (Fig. 4 *E* and *F*). Blocking Rho kinase (ROCK) by using the inhibitor Y27632 (19) also reversed the apical constriction phenotype (Fig. 4*G*), whereas no reversal occurred when a myosin light chain kinase inhibitor, ML7 (19), was added to Dyn2K44A-GFP-expressing cells (Fig. 4*G*). (Phalloidin staining under these conditions is shown in Fig. S3.) Finally, when secramine was added to Dyn2K44A-expressing cells to inhibit Cdc42 GTPase activity (20), apical constriction still occurred (Fig. S4). Hence, Dyn2K44A expression drives apical constriction through a Rho-based, actomyosin contractile system, similar to apical constriction found in other systems (3, 18, 19).

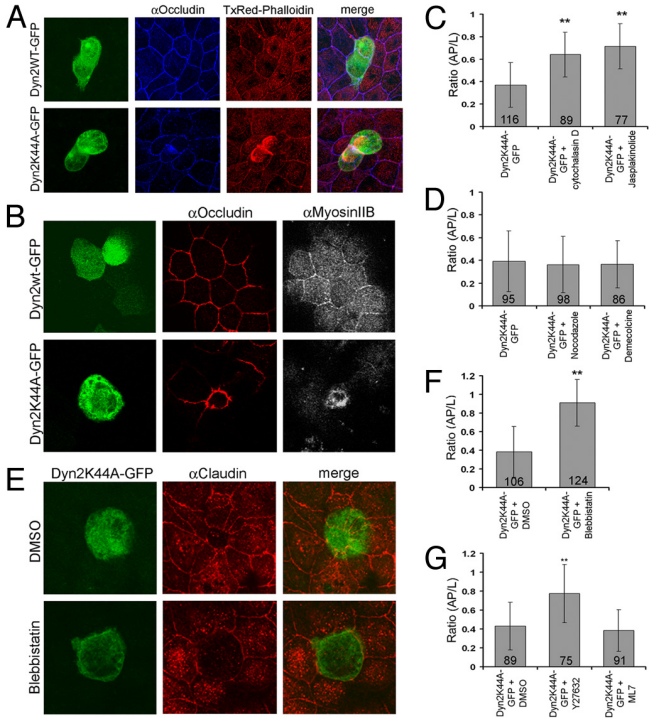

Fig. 4. The actomyosin contractile system is involved in Dyn2K44A-induced apical constriction. (*A*) Maximum intensity projection images of cells expressing Dyn2wt-GFP (*Left Upper*, green) or Dyn2K44A-GFP (*Left Lower*, green) and stained with TxRed-phalloidin (red) and occludin (blue). Note an increase in actin density at the AJC in Dyn2K44A-GFP-expressing cells. (*B*) Single plane images through the AJC of cells expressing Dyn2wt-GFP or Dyn2K44A-GFP and stained for occludin (red) and myosin II (gray). The apical junctional plane of the Dyn2K44A-GFP-expressing cell is above those of untransfected cells. (*C*) Mean ratio (AP/L) of no treatment, cytochalasin D-treated, or jasplakinolide-treated Dyn2K44A-GFP-expressing cells from three independent experiments. **, $P < 0.001$. (*D*) Mean ratio (AP/L) of Dyn2K44A-GFP-expressing cells incubated in 4 °C for 1 h, followed by no treatment, nocodazole treatment, or demecolcine treatment from three independent experiments. (*E*) Maximum intensity projection images of DMSO- or blebbistatin-treated Dyn2K44A-GFP-expressing cells that are stained for claudin (red). Note that inhibiting myosin II with blebbistatin relieves apical constriction. (*F*) Mean ratio (AP/L) of DMSO- or blebbistatin-treated, Dyn2K44A-GFP-expressing cells from four separate experiments. **, $P < 0.001$. (*G*) Mean ratio (AP/L) of DMSO-, Y27632-, or ML7-treated Dyn2K44A-GFP-expressing cells from three independent experiments. **, $P < 0.001$.

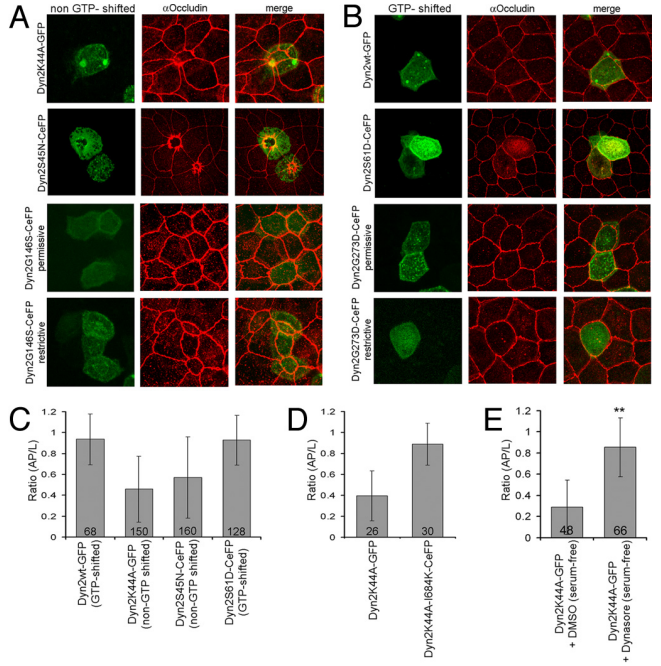

Fig. 5. A shift in nucleotide status dictates dynamin's involvement in apical constriction. (*A*) Maximum intensity projection images of cells expressing Dyn2K44A-GFP, Dyn2S45N-CeFP, and Dyn2G146S-CeFP at 32 °C and Dyn2G146S-CeFP at 40 °C and stained for occludin (red). (*B*) Maximum intensity projection images of cells expressing Dyn2wt-GFP, Dyn2S61D-CeFP, and Dyn2G273D at 32 °C and Dyn2G273D-CeFP at 40 °C (green), and stained for occludin (red). (*C*) Mean ratio (AP/L) of cells expressing Dyn2wt-GFP, Dyn2K44A-GFP, Dyn2S45N-CeFP, and Dyn2S61D-CeFP. (*D*) Mean ratio (AP/L) of cells expressing Dyn2K44A-GFP and Dyn2K44A-I684K-CeFP. (*E*) Mean ratio (AP/L) of DMSO- or dynasore-treated, Dyn2K44A-GFP-expressing cells. **, $P < 0.001$.

Induction of Apical Constriction Relies on the Nucleotide State and GED Domain of Dynamin. To gain insight into whether GTPase-dependent changes in Dyn2 influence actin filament dynamics (21), driving the apical constriction phenotype seen in Dyn2K44A-expressing cells, we examined whether other Dyn2 mutants defective in GTP binding resulted in apical constriction. The mutants tested included: Dyn2S45N, whose amino acid mutation is important for coordinating the α- and β-phosphates of GTP and makes it preferentially shifted to a non-GTP state (22); and the temperature-sensitive Dyn2G146S mutant expressed at its restrictive temperature, predicted to be shifted to a GDP-bound state (23). In the latter case, amino acid G146 was chosen after comparing Dyn2 to the Shibire^{ts2} mutant (23). Notably, both mutants induced apical constriction when expressed in MDCK cells (Fig. 5 *A* and *C*). For Dyn2G146S-GFP, apical constriction only occurred at the restrictive temperature of 40 °C. Interestingly, a Dyn2 mutant containing K44A and I684K (a GED domain mutant) (24) exhibited no apical constriction when expressed in MDCK cells (Fig. 5*D*). This suggested that apical constriction induced by Dyn2K44A and other non-GTP-bound Dyn2 mutants requires some functional aspect of the GED domain within dynamin.

We next examined the effect on monolayer morphology of expressing dynamin mutants shifted to a GTP-bound state. The mutants tested included Dyn2S61D (25) and Dyn2G273D, a temperature-sensitive mutant that is proposed to be shifted to the GTP state at the restrictive temperature (23). Notably, both putative GTP-bound dynamin mutants failed to induce apical constriction when expressed in MDCK cells (Fig. 5 *B* and *C*).

Dynasore, a noncompetitive inhibitor of dynamin that prevents GTP-bound dynamin from undergoing hydrolysis (16), also did not induce apical constriction (Fig. S5). Notably, dynasore treatment relieved apical constriction when added to MDCK cells expressing Dyn2K44A (Fig. 5*E*). One possibility, which remains to be tested, is that by slowing GTP hydrolysis, dynasore acts to slowly shift Dyn2K44A (which has a low affinity for GTP) to a predominantly GTP-bound form. Because pools of GTP-bound dynamin within these cells are now increased (without Dyn2K44A's affinity for GTP having changed), apical constriction is relieved.

Collectively, these results suggest that conditions shifting Dyn2 to its non-GTP-bound state result in more actomyosin contractile activity in the apical circumference zone, whereas conditions shifting Dyn2 to its GTP-bound state result in less actomyosin contractility. Thus, GTPase-dependent changes in Dyn2 seem to regulate actin filament dynamics in polarized cells.

Cortactin's Role in Apical Constriction. Previous work has shown that a complex of Dyn2 and cortactin cross-links actin filaments and forms bundled arrays in vitro (21). Indeed, GTP addition to this complex loosens tightly bundled actin filaments (21). Given this, we investigated whether Dyn2K44A modulates the actomyosin contractile machinery to trigger apical constriction through interactions with cortactin. We coexpressed a cortactin mutant defective in

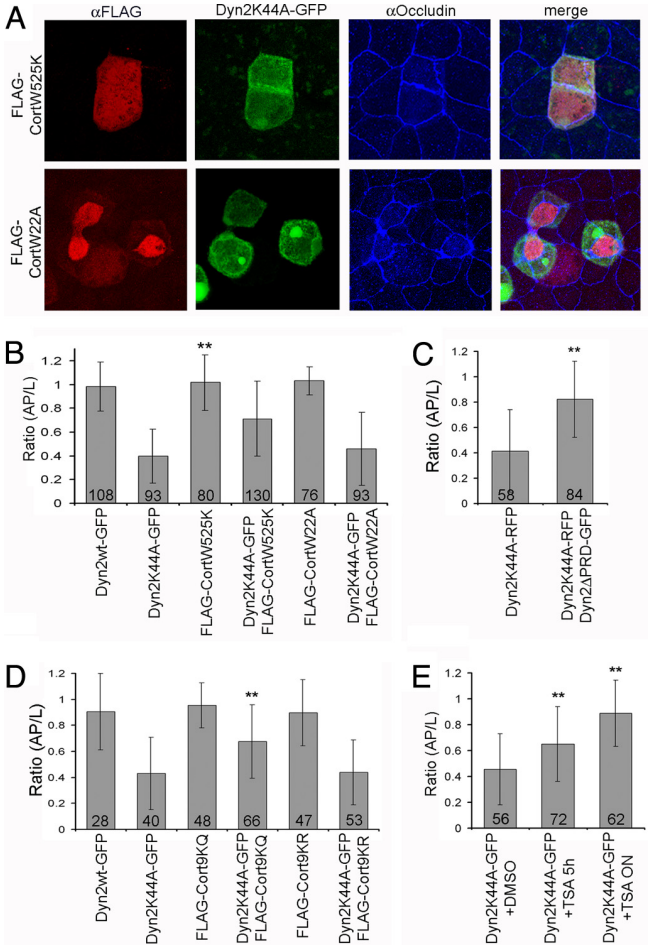

Fig. 6. Testing the role of cortactin and deacetylase in apical constriction induced by Dyn2K44A expression. (*A*) Maximum intensity projection images of Dyn2K44A-GFP-expressing cells cotransfected with FLAG-cortactinW525K (*Upper*) or FLAG-cortactinW22A (*Lower*) and stained for the FLAG tag (red) and occludin (blue). (*B*) Mean ratio (AP/L) for cells expressing Dyn2wt-GFP, Dyn2K44A-GFP, FLAG-cortactinW525K, FLAG-cortactinW22A, Dyn2K44A-GFP and FLAG-cortactinW525K, or Dyn2K44A-GFP and FLAG-cortactinW22A in three independent experiments. **, $P < 0.001$. Note that coexpression of Dyn2K44A-GFP and FLAG-cortactinW525K relieves apical constriction induced by Dyn2K44A. (*C*) Mean ratio (AP/L) for cells expressing Dyn2K44A-RFP only or Dyn2K44A-RFP and Dyn2ΔPRD-GFP in three independent experiments. **, $P < 0.001$. (*D*) Mean ratio (AP/L) for cells expressing Dyn2wt-GFP, Dyn2K44A-GFP, FLAG-Cort9KQ, Dyn2K44A-GFP and FLAG-Cort9KQ, FLAG-Cort9KR, or Dyn2K44A-GFP and FLAG-Cort9KR in two independent experiments. **, $P < 0.001$. Note that coexpression of Dyn2K44A and FLAG-Cort9KQ relieved apical constriction induced by Dyn2K44A. (*E*) Mean ratio (AP/L) for DMSO-treated, TSA-treated (5 h), or TSA-treated (overnight) cells expressing Dyn2K44A-GFP in two independent experiments. **, $P < 0.001$.

dynamin binding (FLAG-cortactin W525K) (26) with Dyn2K44A in MDCK cells. Little or no apical constriction occurred (Fig. 6 *A* and *B*), consistent with Dyn2K44A mediating apical constriction through interactions with cortactin. Further evidence for such a relationship was obtained when we coexpressed Dyn2K44A-RFP and Dyn2ΔPRD-GFP, which lacks the PRD domain important for binding to cortactin (27). No apical constriction was seen (Fig. 6*C*).

Cortactin activation of Arp2/3 stimulates F-actin nucleation and branch assembly during endocytosis (28). To determine whether the apical constriction phenotype depended on Arp2/3 activation, we coexpressed a cortactin mutant defective in activating Arp2/3 (but still capable of binding to dynamin; FLAG-CortactinW22A) (26) with Dyn2K44A-GFP in MDCK cells. Apical constriction still occurred in these cells (Fig. 6 *A* and *B*), suggesting that cortactin's role in Dyn2K44A-induced apical constriction does not depend on its activation of Arp2/3.

Cortactin also regulates the actin cytoskeleton by direct binding to actin (29). Patch charge domains on cortactin are required for this binding, which acetylation of cortactin abrogates. To test whether these patch domains on cortactin are important for the apical constriction phenotype in Dyn2K44A-expressing cells, we coexpressed Dyn2K44A and a myc-tagged cortactin mutant that does not preserve the patch charges (myc-Cort9KQ). No apical constriction occurred (Fig. 6*D*). By contrast, coexpression of Dyn2K44A with the charge-preserving cortactin mutant (myc-Cort9KR) induced apical constriction (Fig. 6*D*). We further found that when we treated MDCK cells expressing Dyn2K44A with trichostatin A (TSA), a general deacetylase inhibitor, to shift cortactin pools to acetylated forms, the apical constriction phenotype was reverted (Fig. 6*E*). Hence, induction of apical constriction in Dyn2K44A-expressing cells may occur through Dyn2K44A–cortactin complexes interacting directly with actin through cortactin's patch charge domains.

Discussion

In this study, we examined Dyn2's role in epithelial morphogenesis. We found that depletion of Dyn2 by siRNA causes polarized epithelial cells to lose their polarity and prevents epithelial cells from polarizing. Expression of Dyn2 mutants shifted to a non-GTP-bound form causes epithelial monolayers to dramatically apically constrict. The formation, maintenance, and modulation of epithelial cell polarity rely on processes dependent on Dyn2 and its GTPase cycle.

Dyn2 regulation of epithelial morphogenesis could function through an endocytic role (9). Previous studies have shown that components of the apical junctional region continually turn over through endocytosis (6). Our finding that Dyn2 dynamically localizes to membranes in the apical junctional region (moving on and off membranes) and that tight junctional proteins mislocalize and polarity is lost upon Dyn2 depletion suggests a dynamin-mediated endocytic pathway spatially regulates the distribution of junctional proteins and their binding partners. A similar role for dynamin-dependent endocytosis has been proposed for maintaining polarity factors at the anterior pole of the developing *Caenorhabditis elegans* embryo (30).

However, our studies suggest there is an additional mechanism, not dependent on endocytosis, whereby Dyn2 regulates epithelial morphogenesis. This is by modulating the actomyosin contractile apparatus in the junctional region. Evidence suggesting this came from experiments showing cells undergo apical constriction when Dyn2 mutants shifted to non-GTP forms (i.e., Dyn2K44A) are expressed. This phenotype depends on Rho kinase and myosin II activity and is not due to Dyn2K44A's inhibitory effect on endocytosis, because other endocytic inhibitors (i.e., Eps15Δ95/295 and Cav1Y14F) do not induce apical constriction. Instead, the effect is due to GTPase-dependent changes in Dyn2, in conjunction with cortactin, for modulation of the actomyosin contractile apparatus in the junctional region.

Cortactin is an actin-binding protein that is the target of multiple kinases and serves as a central element connecting signaling pathways with cytoskeletal restructuring (28, 31). It also binds to ZO-1 and may participate in the organization of tight junctions and adherens junctions (28, 31). Furthermore, cortactin stimulates Dyn2's intrinsic GTPase activity and stabilizes the association of Dyn2 and actin filaments (21). Evidence for cortactin's role in mediating apical constriction induced by Dyn2K44A came from our finding that a cortactin mutant defective in dynamin binding, when coexpressed with Dyn2K44A, prevents apical constriction.

A complex of dynamin and cortactin has been shown previously to modulate actin dynamics in work by Schafer and colleagues (21). They showed that dynamin–cortactin complexes can directly cross-

link actin filaments to form bundled arrays in vitro. Because patch charge domains on cortactin are required for direct binding with actin filaments (29), we tested the effect of removing these domains on apical constriction induced by Dyn2K44A. We found no constriction occurs, favoring the view that dynamin–cortactin complexes bind and cross-link actin during apical constriction. Exactly how dynamin–cortactin complexes direct actin filamant bundling to drive apical constriction during Dyn2K44A expression remains to be investigated. It is possible that GTPase-dependent changes within Dyn2 transduce via cortactin to directly remodel actin. Alternatively, actin could be indirectly remodeled via dynamin and cortactin interactions with other proteins that regulate actin filament assembly, filament stabilization, or filament organization. Whatever the mechanism, what is clear is that the organization and dynamics of actin filaments associated with actomyosin contractile bundles in Dyn2K44A-expressing cells are regulated by dynamin–cortactin complexes. These complexes may therefore influence the global organization of the actomyosin cytoskeleton in polarized cells.

The dual role of Dyn2 in endocytosis and actomyosin dynamics in the junctional region of polarized cells suggested in this study raises the question of how dynamin's activity is modulated for triggering endocytosis versus actomyosin contraction. Schafer and colleagues (21) have shown in in vitro studies that non-GTP-bound dynamin preferentially complexes with cortactin in tightly bundled actin filaments (21). This fits well with our finding that only Dyn2 mutants shifted to a non-GTP-bound state cause apical constriction in polarized MDCK cells. A model can thus be proposed in which dynamin's overall nucleotide state underlies its dual role in endocytosis versus actomyosin dynamics in polarized cells. In this view, despite overall GTP levels within cells being high, levels of dynamin in different nucleotide states vary geographically within the cell because of local conditions that modulate dynamin's GTPase cycle. Thus, when local concentrations of Dyn2-GTP at the apical junctional area are high, effectors are recruited that drive endocytic membrane activity. Likewise, when local concentrations of Dyn2-GTP are low, effectors are recruited that modulate the actomyosin contractile machinery. In this way, Dyn2 would regulate endocytosis and actomyosin contractility in the apical junctional region for biogenesis and morphogenesis of polarized epithelial cells.

Materials and Methods

Cell Culture. MDCKII cells were maintained in MEM with 4 mM L-glutamine and 10% FBS at 37 °C with 5% CO_2 levels. Cells were interchangeably cultured on the inside or the outside of Transwells (12). Cells seeded at a density of 1×10^5 on 12-mm Transwells (Corning) reached 100% confluency in 2 days. siRNA-treated, suspended MDCK cells seeded at a density of 4×10^6 reached 100% confluency immediately. Monolayers were cultured for an additional 3 days after reaching confluency.

Plasmids, siRNA, and Transfection. See *SI Methods* for details.

Protein Analysis. See *SI Methods* for details.

Primary Antibodies and Reagents. See *SI Methods* for details.

Immunofluorescence Staining, Confocal Fluorescence Imaging, and Data Analysis. Monolayers were fixed with paraformaldehyde (4%, 15 min) and permeabilized with saponin (0.01%, 15 min) and incubated in primary antibody followed by secondary antibody conjugated to a fluorophore. The porous filters were excised and mounted onto a glass slide by using Fluoromount G (Electron Microscopy Sciences).

Confocal scanning microscopy was performed on the Zeiss Meta LSM 510 confocal system. Images were taken with a 63×1.4 N.A. Apochromat oil immersion objective lens (Carl Zeiss) with a pinhole set to 1 airy unit. Image processing was performed by using Zeiss LSM 5 image examiner and Photoshop 7.0 (Adobe Systems). All maximum intensity projection images were all cropped to 50×50 μm, except for siRNA-treated images, which were cropped to 100×100 μm. Movies were processed by using Volocity 4.0 software (Improvision).

Data analysis was performed by using Image J software (National Institutes of Health, Bethesda, MD), and Microsoft Excel was used to generate bar graphs. Numbers of bar graphs denote the number of cells counted (n). Statistical analysis was performed in GraphPad, and error bars denote SD.

Fluorescence Recovery After Photobleaching (FRAP) and Live Cell Imaging. FRAP experiments were performed on a Zeiss Confocor LSM 510 confocal system. Temperature was maintained at 37 °C by using an ASI 400 Air Stream Incubator (NEVTEK). Live cell imaging was performed on the Ultraview ERS system (Perkin–Elmer) using the same objective lens as stated previously.

ACKNOWLEDGMENTS. We thank Dylan Burnette, Natalie Elia, Jenny Hinshaw, and Ramanujan Hegde for invaluable insights, discussions, and readings.

1. Lecuit T, Lenne PF (2007) Cell surface mechanics and the control of cell shape, tissue patterns and morphogenesis. *Nat Rev Mol Cell Biol* 8:633–644.
2. Wallingford JB (2005) Neural tube closure and neural tube defects: Studies in animal models reveal known knowns and known unknowns. *Am J Med Genet C Semin Med Genet* 135C:59–68.
3. Dawes-Hoang RE, et al. (2005) Folded gastrulation, cell shape change and the control of myosin localization. *Development* 132:4165–4178.
4. Hartsock A, Nelson WJ (2008) Adherens and tight junctions: Structure, function and connections to the actin cytoskeleton. *Biochim Biophys Acta* 1778:660–669.
5. Lecuit T, Wieschaus E (2002) Junctions as organizing centers in epithelial cells? A fly perspective. *Traffic* 3:92–97.
6. Ivanov AI, Nusrat A, Parkos CA (2005) Endocytosis of the apical junctional complex: mechanisms and possible roles in regulation of epithelial barriers. *Bioessays* 27:356–365.
7. Schafer DA (2004) Regulating actin dynamics at membranes: A focus on dynamin. *Traffic* 5:463–469.
8. Praefcke GJ, McMahon HT (2004) The dynamin superfamily: Universal membrane tubulation and fission molecules? *Nat Rev Mol Cell Biol* 5:133–147.
9. Orth JD, McNiven MA (2003) Dynamin at the actin-membrane interface. *Curr Opin Cell Biol* 15:31–39.
10. Sweitzer SM, Hinshaw JE (1998) Dynamin undergoes a GTP-dependent conformational change causing vesiculation. *Cell* 93:1021–1029.
11. Damke H, Baba T, Warnock DE, Schmid SL (1994) Induction of mutant dynamin specifically blocks endocytic coated vesicle formation. *J Cell Biol* 127:915–934.
12. Wakabayashi Y, Chua J, Larkin JM, Lippincott-Schwartz J, Arias IM (2007) Four-dimensional imaging of filter-grown polarized epithelial cells. *Histochem Cell Biol* 127:463–472.
13. Martin-Belmonte F, et al. (2007) PTEN-mediated apical segregation of phosphoinositides controls epithelial morphogenesis through Cdc42. *Cell* 128:383–397.
14. Benmerah A, Bayrou M, Cerf-Bensussan N, Dautry-Varsat A (1999) Inhibition of clathrin-coated pit assembly by an Eps15 mutant. *J Cell Sci* 112:1303–1311.
15. del Pozo MA, et al. (2005) Phospho-caveolin-1 mediates integrin-regulated membrane domain internalization. *Nat Cell Biol* 7:901–908.
16. Macia E, et al. (2006) Dynasore, a cell-permeable inhibitor of dynamin. *Dev Cell* 10:839–850.
17. Henley JR, McNiven MA (1996) Association of a dynamin-like protein with the Golgi apparatus in mammalian cells. *J Cell Biol* 133:761–775.
18. Martin AC, Kaschube M, Wieschaus EF (2009) Pulsed contractions of an actin-myosin network drive apical constriction. *Nature* 457:495–499.
19. Hildebrand JD (2005) Shroom regulates epithelial cell shape via the apical positioning of an actomyosin network. *J Cell Sci* 118:5191–5203.
20. Pelish HE, et al. (2006) Secramine inhibits Cdc42-dependent functions in cells and Cdc42 activation in vitro. *Nat Chem Biol* 2:39–46.
21. Mooren OL, Kotova TI, Moore AJ, Schafer DA (2009) Dynamin2 GTPase and cortactin remodel actin filaments. *J Biol Chem* 284:23995–24005.
22. Marks B, et al. (2001) GTPase activity of dynamin and resulting conformation change are essential for endocytosis. *Nature* 410:231–235.
23. Narayanan R, Leonard M, Song BD, Schmid SL, Ramaswami M (2005) An internal GAP domain negatively regulates presynaptic dynamin in vivo: A two-step model for dynamin function. *J Cell Biol* 169:117–126.
24. Soulet F, Schmid SL, Damke H (2006) Domain requirements for an endocytosis-independent, isoform-specific function of dynamin-2. *Exp Cell Res* 312:3539–3545.
25. Song BD, Leonard M, Schmid SL (2004) Dynamin GTPase domain mutants that differentially affect GTP binding, GTP hydrolysis, and clathrin-mediated endocytosis. *J Biol Chem* 279:40431–40436.
26. Schafer DA, et al. (2002) Dynamin2 and cortactin regulate actin assembly and filament organization. *Curr Biol* 12:1852–1857.
27. McNiven MA, et al. (2000) Regulated interactions between dynamin and the actin-binding protein cortactin modulate cell shape. *J Cell Biol* 151:187–198.
28. Cosen-Binker LI, Kapus A (2006) Cortactin: The gray eminence of the cytoskeleton. *Physiology (Bethesda)* 21:352–361.
29. Zhang X, et al. (2007) HDAC6 modulates cell motility by altering the acetylation level of cortactin. *Mol Cell* 27:197–213.
30. Nakayama Y, et al. (2009) Dynamin participates in the maintenance of anterior polarity in the Caenorhabditis elegans embryo. *Dev Cell* 16:889–900.
31. Ammer AG, Weed SA (2008) Cortactin branches out: Roles in regulating protrusive actin dynamics. *Cell Motil Cytoskeleton* 65:687–707.